BNL 31989
INFORMAL REPORT

BNL--31989

DE83 001731

AN OVERVIEW OF UNDULATORS AND WIGGLERS FOR THE NSLS

S. Krinsky, W. Thomlinson, A van Steenbergen

September 1982

Research Supported by the
OFFICE OF BASIC ENERGY SCIENCES
U.S. DEPARTMENT OF ENERGY
WASHINGTON, D.C.

BROOKHAVEN NATIONAL LABORATORY
UPTON, NEW YORK 11973

I. INTRODUCTION

This summary is designed to present to the NSLS user community the possible options for wigglers and undulators. The desire is to make it possible for every user to respond to the request by the NSLS for guidance in insertion device development so that it can best serve their scientific interests. There are many options, each with its own advantages and disadvantages, as well as certain restrictions imposed by the parameters of the NSLS storage rings. At the Users Meeting held in May 1982, Sam Krinsky and Arie van Steenbergen presented some of the options and the reasoning behind certain choices. Their presentations have been rearranged and expanded to form this paper. Useful references for the nonexpert are the recent Physics Today article by Winick, et al.[1] and Jackson's treatment in his book Classical Electrodynamics.[2]

The NSLS is asking for input in two areas. First, we must decide on the instrumentation to be developed for the high field superconducting wiggler beam lines and for the hybrid permanent magnet wiggler lines. These two devices are currently being constructed and will be installed during the next half year on the x-ray ring. The types of beam lines connected to them must be determined; i.e. whether they will be spectroscopy or scattering lines, focused or unfocused, etc. This input from the users is needed immediately.

Secondly, the long-range plans for additional insertion devices are now under discussion. Choices must soon be made between the large number of different magnets which can be built. On the x-ray ring there are seven straight sections that can accept wigglers or undulators, and on the

VUV ring there are two such insertions, one of which is currently occupied by the Free Electron Laser experiment. It is our hope that users will now communicate to us their ideas and preferences relating to wiggler and undulator development.

To facilitate user response, we provide a review of the properties of wigglers and undulators in Section II, introducing the basic concepts[3] and defining the fundamental parameters. A detailed account of the brightness of the undulator source is presented in Section III. Next, the insertion devices already under construction for the x-ray and VUV rings are discussed in Sections IV and V, respectively. In Section VI, we describe the suitability of certain proposed undulators for the generation of soft x-rays (5-50Å, Section VIA) and harder x-rays (3-12Å, Section VIB). Some concluding remarks are given in Section VII.

At the end of Sections IV, V, VI.A, VI.B, we place figures and tables describing the properties of the specific devices discussed in the text, preceded by a page containing descriptive captions. The figures pertaining to the review sections II and III are more informally incorporated into the discussion.

II. REVIEW OF THE PROPERTIES OF WIGGLERS AND UNDULATORS

A wiggler magnet is located in a straight section of the storage ring, its axis being parallel to the unperturbed electron motion (z-direction). The wiggler produces a vertical magnetic field B_y, which has a period length λ_o in the z-direction, and to a good approximation is sinusoidal,

$$B_y = B_o \sin(2\pi z/\lambda_o) \ . \tag{1}$$

The magnetic field causes the electrons to be deflected in the horizontal plane, and we denote this deflection x. Consider the electrons to have energy γ, measured in units of their rest mass, and let ρ_o denote the radius of curvature corresponding to the peak field B_o. The angular deflection, $x' = dx/dz$, of the electrons is

$$x' = \frac{K}{\gamma} \cos(2\pi z/\lambda_o) \ , \tag{2}$$

where the magnetic strength parameter K is defined by

$$\frac{K}{\gamma} = \frac{\lambda_o}{2\pi\rho_o} \ , \tag{3}$$

and a useful approximation is

$$K \approx 0.93 \ B_o(\text{Tesla})\lambda_o(\text{cm}). \tag{4}$$

Clearly, K/γ is the maximum angular deflection of the electrons and $(\lambda_o/2\pi)(K/\gamma)$ is the amplitude of the transverse oscillation. The magnitude of the electron velocity divided by the speed of light is $\beta = \sqrt{1 - \gamma^{-2}}$. Due to the transverse deflection, the average velocity β^* in the z-direction is reduced from the value β, and is approximately

$$\beta^* = \beta\left(1 - \frac{K^2}{4\gamma^2}\right) \ . \tag{5}$$

Consider a wavefront radiated by an electron passing through the periodic magnetic field. At time $\lambda_o/\beta^* c$ later, the electron has passed through one period of the magnet, and a second wavefront radiated at this time will follow the first by a time interval

$$T_1 = \frac{\lambda_o}{\beta^* c} - \frac{\lambda_o}{c} . \tag{6}$$

Hence, an observer downstream of the magnet looking in the forward direction will observe a radiation spectrum composed of the fundamental frequency $\omega_1 = 2\pi/T_1$ and its harmonics $\omega_k = k\omega_1 (k = 1,3,5..)$. The fundamental wavelength $\lambda_1 = cT_1$ can be expressed as

$$\lambda_1 = \frac{\lambda_o}{2\gamma^2} \left(1 + \frac{K^2}{2}\right) , \tag{7}$$

where we have used the fact that γ is much larger than unity. If the observer is looking at radiation emitted at (polar) angle θ relative to the z-axis, then the time delay between wavefronts emitted before and after an electron has traversed one period of the magnetic field is

$$T_1(\theta) = \frac{\lambda_o}{\beta^* c} - \frac{\lambda_o \cos\theta}{c} . \tag{8}$$

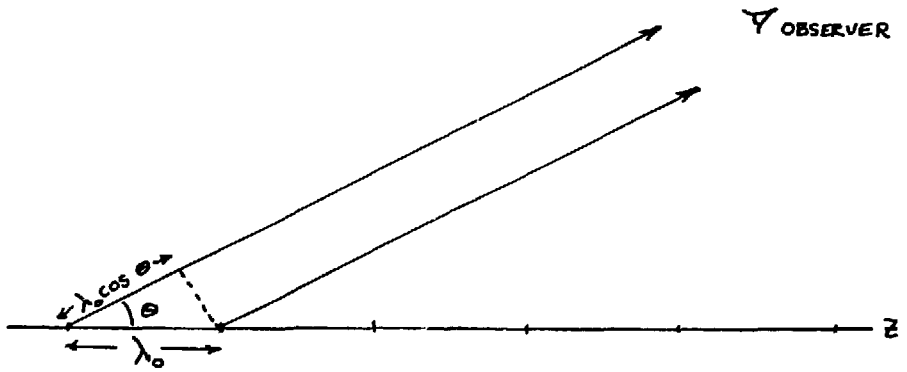

The corresponding fundamental wavelength is

$$\lambda_1(\theta) = \frac{\lambda_o}{2\gamma^2}\left(1 + \frac{K^2}{2} + \gamma^2\theta^2\right) . \tag{9}$$

For a magnet with N periods, we see that the radiated pulse from one electron passing through the device has a time duration NT_1, so the pulse contains Nk radiation periods at the kth harmonic frequency ω_k(k=1,2,3..). Consequently, the line width at fixed observation angle θ is

$$\frac{\Delta\omega_k}{\omega_k} \simeq \frac{1}{kN} . \tag{10}$$

Due to the dependence of the frequency on observation angle θ, if the observer accepts radiation in an interval $\Delta\theta$, then the width of the line is broadened relative to its natural value [Eq. (10)]. From Eq. (9), we see that the angular broadening due to accepting radiation in a cone of half-angle $\Delta\theta$ about the forward direction is

$$\frac{\Delta\omega_k}{\omega_k} = \frac{\gamma^2(\Delta\theta)^2}{1 + \frac{K^2}{2}} . \tag{11}$$

The broadening will be small only if

$$\Delta\theta \lesssim \frac{1}{\gamma}\sqrt{\frac{1 + \frac{K^2}{2}}{2kN}} . \tag{12}$$

Note from Eq. (9), that the radiation becomes softer as the observer moves away from the forward direction. This results in a broadening of the low frequency side of the line, but the high frequency side remains sharp.

In the forward direction, radiation from a wiggler is in general characterized by two time scales. The first is the time interval T_1 of Eq. (6), and the second is the time characteristic of synchrotron radiation T_c,

$$T_c = \frac{4\pi}{3} \frac{\rho_o}{c} \frac{1}{\gamma^3} . \tag{13}$$

When the magnetic strength parameter $K \gg 1$, then $T_1 \gg T_c$, and the time dependence of the radiated electric field has the form[4]:

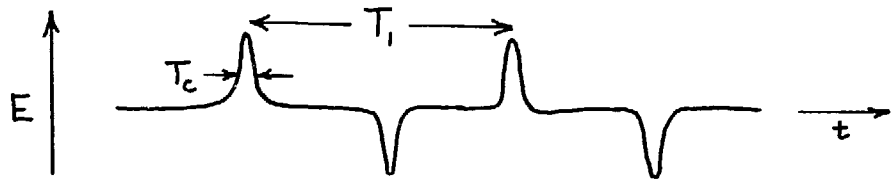

For high harmonic number k, the frequency spectrum is characterized by the synchrotron radiation cutoff frequency $\omega_c = 2\pi/T_c$. From Eq. (13) it is seen that the critical energy $\varepsilon_c \propto BE^2$, where B is the magnetic field and E is the energy of the electrons.

We denote the energy radiated per unit solid angle, per unit frequency interval by $dI(\omega)/d\Omega$. For a wiggler with N periods,[5]

$$\left.\frac{dI(\omega)}{d\Omega}\right|_{\substack{\theta = 0 \\ \omega = k\omega_1}} = \frac{e^2N^2\gamma^2}{c} F_k(K) \ , \quad (k = 1,3,5\ldots) \tag{14}$$

where $F_k(K)$ is computable in terms of Bessel functions [see Eq. (34) of Sect. III] for the sinusoidal field of Eq. (1). In the limit $K \to \infty$, $k \to \infty$, with k/K^3 held fixed,

$$F_k(K) \approx \frac{3}{\pi^2} \left(\frac{k}{k_c}\right)^2 K_{\frac{2}{3}}^2 \left(\frac{k}{2k_c}\right) , \tag{15}$$

$$k_c = \frac{3}{8} K^3 , \tag{16}$$

and $\omega_c = k_c\omega_1$. Substituting in (14) and comparing with results from Jackson,[2] one obtains the result,

$$\left.\frac{dI(\omega)}{d\Omega}\right|_{\substack{\text{wiggler} \\ \theta = 0 \\ \omega = k\omega_1}} = (2N)^2 \left.\frac{dI(\omega)}{d\Omega}\right|_{\substack{\text{synchrotron} \\ \text{radiation} \\ \theta = 0 \\ \omega = k\omega_1}} \tag{17}$$

Radiation in this regime is called "wiggler" radiation.

When the field strength parameter $K \lesssim 1$, then $T_1 < T_c$, and the time scale T_c characteristic of synchrotron radiation drops out of the problem. In this case one usually speaks of "undulator" radiation[6] rather than "wiggler" radiation. For an undulator, the time dependence of the electric field in the forward direction has the form

For $K \ll 1$, the electric field has almost a purely sinusoidal time dependence, and hence the radiation spectrum is dominated by the line at the fundamental frequency ω_1. When K increases toward unity, the third harmonic becomes important, corresponding in the time domain to a sharpening of the peak of the electric field. Clearly, as K increases toward higher values the higher harmonics increase, corresponding to well-defined pulses of width T_c separated by time T_1.

We can compare the angle integrated spectrum of undulator radiation with that of synchrotron radiation. For an undulator, the peak value of the integrated spectrum at the fundamental frequency is [photons/sec, $(\Delta\omega/\omega)$, I(Amp)]:

$$\eta_u(\omega_1) \simeq \frac{\pi\alpha\, NK^2}{1 + (K^2/2)} \frac{I}{e} \frac{\Delta\omega}{\omega} , \qquad (18)$$

where $e = 1.6 \times 10^{-19}$ Coul. is the electron charge, I is the electron beam current in Amperes, and $\alpha = 1/137$ is the fine structure constant. Note that although the value of the fundamental frequency ω_1 depends on the electron energy γ, the peak height $\eta_u(\omega_1)$ is independent of γ.

For a bending magnet, the integrated spectrum at the critical frequency ω_c is $\left[\text{photons/sec}, \frac{\Delta\omega}{\omega}, \theta(\text{mrad}), I(\text{Amp})\right]$:

$$\eta_B(\omega_c) = 0.65 \frac{\sqrt{3}}{2\pi} \alpha \gamma \frac{\Delta\omega}{\omega} \frac{I}{e} \theta \times 10^{-3} . \qquad (19)$$

Here, $\eta_B(\omega_c)$ is seen to be proportional to the energy γ, in contrast to the case of the undulator.

One often differentiates between wigglers and undulators by the magnitude of the magnetic strength parameter K. That is, undulator radiation characterized by the radiation being concentrated in discrete harmonics is produced when $K \lesssim 1$. For $K \gg 1$ the radiation spectrum is that of synchrotron radiation and is characteristic of wigglers. From Eq. (4) it is clear that undulator radiation is produced by devices which have low fields and short magnetic periods.

Use of wigglers is the only way of obtaining photons with energies greater than 30 keV at the NSLS. For the x-ray ring operating at 2.5 GeV, the critical wavelength is related to the magnetic field by

$$\lambda_c(\text{Å}) = 3/B(T). \tag{20}$$

The 1.2 T bending magnets yield λ_c = 2.5 Å, while a 6 T wiggler produces λ_c = 0.5 Å. The flux per unit solid angle from a wiggler is 2N times that from an arc source of the same field strength, and the radiation is collimated in the horizontal plane with the full horizontal opening angle

$$2\theta_{1/2} = 2\ K/\gamma. \tag{21}$$

The effective source size ℓ_x depends on the observation angle θ, and for a wiggler of length L,

$$\ell_x \approx L\theta/2. \tag{22}$$

Because of the variation [Eq. (1)] of the magnetic field strength in a wiggler, the effective critical wavelength also depends on θ. Radiation within an angle of $\pm$ 0.6 K/γ of the forward direction will have a 20% variation in critical wavelength.

For the NSLS x-ray ring at 2.5 GeV the total power radiated by a device of length L(m), field B(T), and electron current I(A) is

$$P(kW) = 3.9\ B^2LI. \tag{23}$$

Writing this in terms of the device parameters K, λ_o(cm), and N (no. of periods)

$$P(kW) = 0.045\ \frac{K^2NI}{\lambda_o} \tag{24}$$

The wigglers have a substantial power output. The superconducting wiggler at the NSLS radiates about 1 kW/horizontal milliradian. On the other hand, undulators radiate considerably less total integrated power, even

though they are highly collimated, high flux sources. For example, an undulator on the x-ray ring with K = 0.5, λ_o = 6 cm, I = 0.5 A and N = 50 radiates 47 W into a horizontal angle of ~ 0.4 mrad.

For undulators ($K \lesssim 1$) the spectrum consists of a series of harmonic peaks ($\omega_k = k\omega_1$) with the undulator radiation concentrated in a few harmonics. The flux is highly collimated in the horizontal plane with $2\theta_{1/2} \sim 2/\gamma$. The enhancement of the flux per unit solid angle over that from a bending magnet depends on how much variation there is in the direction of motion of the electrons in the stored beam passing through the undulator. As discussed in Section III, if the electrons move on trajectories which are sufficiently parallel, then the radiated wavelength is correlated to the observation angle, and the undulator flux per $(\text{mrad})^2$ per $\Delta\lambda/\lambda$ is enhanced a factor of N^2. The importance of the high collimation is that there is a very efficient collection of radiation and a high ratio of useful photons to the total power in the beam.

We can compare[7] the angle integrated flux (vertical and horizontal) at the first harmonic of an undulator (N_u, K_u) with the flux from 1 mrad of an arc source at the critical frequency ω_c:

$$\frac{\eta_u(\omega_1)}{\eta_B(\omega_c)} \sim 17500 \quad \frac{NK^2}{\gamma[1 + (K^2/2)]} \tag{25}$$

for the same bandwidth $\Delta\omega/\omega$. For the NSLS rings, γ(x-ray) = 4900 and γ(vuv) = 1370. As an example take N = 100, K = 1, and γ = 4900, then the flux radiated into about 0.6 mrad horizontal by the undulator is 238 times that radiated into 1 mrad by the bending magnet.

Comparing an undulator with a wiggler (N_w, B_w, θ_w), the integrated flux ratio is

$$\frac{\eta_u(\omega_1)}{\eta_w(\omega_c)} \approx \frac{N_u}{N_w \theta_w} \frac{1.8\ K_u^2}{[1 + (K_u^2/2)]} \tag{26}$$

where θ_w mrad of radiation is collected from the wiggler, and all the angle integrated flux at ω_1, is collected from the undulator.

III. THE BRIGHTNESS OF THE UNDULATOR SOURCE

In the preceeding section we have considered the total angle integrated flux (photons/sec, unit bandwidth) as in Eqs. 18, 19, 25 and 26 and the flux per unit solid angle (photons/sec, steradian, unit bandwidth) as in Eqs. 14-17. For experiments which require a photon beam with small angular deviation incident upon a small sample, the true figure of merit of a source is its "brightness", i.e. the flux per unit phase space volume (photons/sec/steradian/mm^2/unit bandwidth).

To understand the phase space of the undulator source it is necessary to discuss some of the fundamentals of the electron beam optics.[8] The transverse dimensions and the angular spread of the electron beam in an insertion are determined by the emittances ε_x, ε_y of the storage ring, and the local values of the betatron functions $\beta_x(s)$ and $\beta_y(s)$. Here, x denotes the radial direction and y the vertical. (In the following equations if ε or $\beta(s)$ appears without a subscript, the equation is to be understood as holding separately for x and y.)

Within an insertion, the betatron functions have the form

$$\beta(s) = \beta^* + \frac{s^2}{\beta^*} , \tag{27}$$

where s is the distance from the insertion center s = 0. The electron beam size is given by

$$\sigma(s) = \sqrt{\varepsilon\beta(s)} , \tag{28}$$

and the angular spread,

$$\sigma'(s) = \sqrt{\varepsilon/\beta^*} \equiv \sigma' . \tag{29}$$

At the insertion center,

$$\sigma\sigma' = \varepsilon, \tag{30}$$

and off-center

$$\sigma(s) = \sqrt{\sigma^2 + (\sigma' s)^2} \ . \tag{31}$$

Consider an observer viewing radiation from an undulator situated in the insertion, and accepting only radiation emitted along the undulator axis. If there were no angular spread in the electron beam, then the observed radiation would have a line width $\Delta\omega_k/\omega_k = (kN)^{-1}$ for the k-th harmonic. When there is angular spread σ', the line is broadened as in the case of a spread in observation angle $\Delta\theta$ [Eq. (11)], and the broadening is small only if

$$\sigma' \lesssim \sigma'_R \equiv \frac{1}{\gamma\sqrt{2kN}} \left(1 + \frac{K^2}{2}\right)^{1/2} \ . \tag{32}$$

In the absence of angular spread in the electron beam, the central intensity of the kth odd harmonic at frequency ω_k is

$$\left.\frac{dI(\omega_k)}{d\Omega}\right|_{\theta=0} = \alpha N^2 \gamma^2 \frac{\Delta\omega}{\omega} \frac{I}{e} F_k(K) \ , \tag{33}$$

expressed in [photons/sec, steradian, $\Delta\omega/\omega$, I(Amperes)]. As in Eq. (18), $\alpha = 1/137$ is the fine structure constant and $e = 1.6 \times 10^{-19}$ Coul. The function $F_k(K)$ appeared earlier in Eq. (14), and is explicitly given by[5]

$$F_k(K) = \frac{K^2 k^2}{\left(1 + \frac{K^2}{2}\right)^2} \left[J_{\frac{k+1}{2}}\left(\frac{kK^2}{4 + 2K^2}\right) - J_{\frac{k-1}{2}}\left(\frac{kK^2}{4 + 2K^2}\right)\right]^2 \tag{34}$$

and the values of $F_k(K)$ for k = 1,3 and 5 are presented in Fig. 3.1.

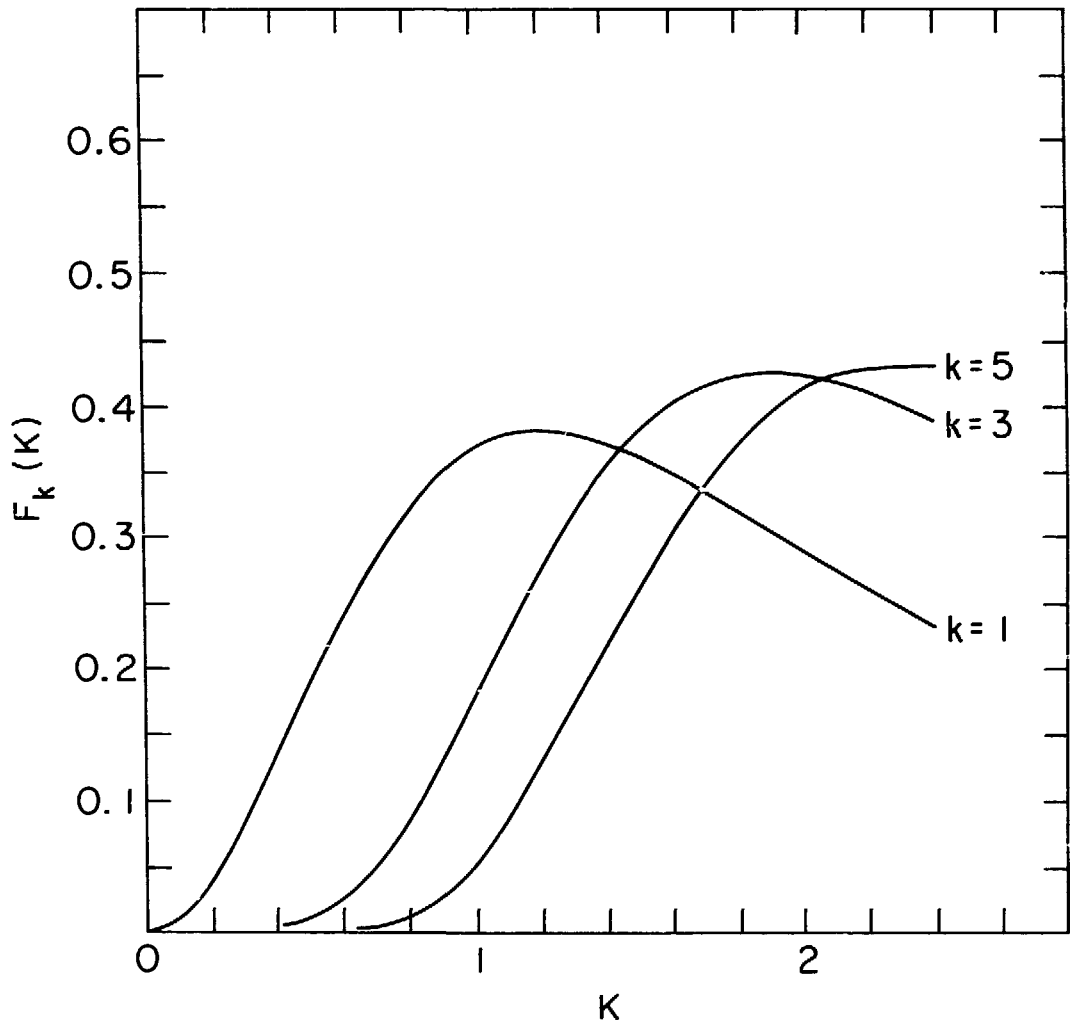

Fig. 3.1

It is interesting to rewrite Eq. (33) as

$$\left.\frac{dI(\omega_k)}{d\Omega}\right|_{\theta=0} = \frac{\eta_k}{2\pi\sigma_R'^2} , \tag{35}$$

where σ_R' was defined in Eq. (32) and

$$\eta_k = \pi\alpha N \left(1 + \frac{K^2}{2}\right) \frac{1}{k} F_k(K) \frac{\Delta\omega}{\omega} \frac{I}{e} \tag{36}$$

is the contribution from the kth harmonic to the angle integrated intensity at frequency ω_k, expressed in [photons/sec, $\Delta\omega/\omega$, I(Ampere)]. For small K, η_k is approximately equal to the total angle integrated flux at frequency ω_k, but for larger K, harmonics higher than the kth also contribute. In the case of the first harmonic, k = 1, and small K,

$$F_1(K) \approx K^2/\left(1 + \frac{K^2}{2}\right)^2 ,$$

so Eq. (36) is seen to reduce to Eq. (18).

Now suppose the electron beam to have angular spread $\sigma'_{x,y}$ where the subscript indicates the x and y values independently. Inspection of Eq. (35) suggests that σ_R' is the rms angular spread of the undulator radiation with frequency ω_k. Following the approach taken by G.K. Green[9] in his treatment of synchrotron radiation from a bending magnet, we would expect that Eq. (35) is replaced by

$$\left.\frac{dI(\omega_k)}{d\Omega}\right|_{\theta=0} = \frac{\eta_k}{2\pi\Sigma'_x\Sigma'_y} \tag{37}$$

where

$$\Sigma'_{x,y} = \sqrt{\sigma'^2_R + \sigma'^2_{x,y}} \tag{38}$$

The subscript x,y means that the equation holds independently for x and y. This approach is heuristic since the angular distribution of undulator radiation is not truly Gaussian, but we would expect the qualitative features illustrated by the following discussion to be correct.

The effective size $\Sigma_{x,y}$ of the undulator source depends on its length $L = N\lambda_o$, and again following G.K. Green[9] we assume

$$\Sigma_{x,y} = \sqrt{\sigma^2_{x,y} + (\sigma'^2_R + \sigma'^2_{x,y})\frac{L^2}{4}} \,. \tag{39}$$

The brightness B_k of the undulator at frequency ω_k is

$$B_k = \frac{1}{2\pi\Sigma_x\Sigma_y}\left.\frac{dI(\omega_k)}{d\Omega}\right|_{\theta=0'} \tag{40}$$

which can be rewritten using Eqs. (37) and (38) as

$$B_k = \frac{\eta_k}{4\pi^2\Sigma_x\Sigma'_x\Sigma_y\Sigma'_y} \tag{41}$$

where η_k is defined in Eq. (36).

It is interesting to note that

$$\sum_{x,y}\sum'_{x,y} \geq \left(\sigma^2_{x,y} + \frac{L^2}{4}\,\sigma'^2_R\right)^{1/2} \sum'_{x,y} \geq \varepsilon_{x,y} + \frac{\lambda_k}{2}\,, \qquad (42)$$

where the emittances $\varepsilon_{x,y}$ were defined in Eq. (30), and we have used

$$\lambda_k = \sigma'^2_R L = \frac{\lambda_o}{2k\gamma^2}\left(1 + \frac{K^2}{2}\right)\,, \qquad (43)$$

with σ_R' defined in Eq. (32). The inequality (42) has the form of a diffraction limit on the phase space of the photon source, and implies an upper bound on the brightness of an undulator,

$$B_k \leq \frac{\mathcal{N}_k}{\pi^2\lambda_k^2} \qquad (44)$$

Let us now consider two examples which illustrate the effect of the values of the beta-functions on the undulator brightness.

Example 1. High-Beta Insertion:

$$\sigma'_{x,y} \approx \sigma'_R \qquad (45)$$

$$\sigma'_R \frac{L}{2} \ll \sigma_{x,y} \qquad (46)$$

Together, (45) and (46) imply

$$\beta^*_{x,y} = \frac{\sigma_{x,y}}{\sigma'_{x,y}} \gg \frac{L}{2} \tag{47}$$

$$\varepsilon_{x,y} \gg \lambda_k/2 \tag{48}$$

where we have used Eqs. (29), (30), and (43).

In this case

$$\sum_{x,y} \approx \sigma_{x,y} \text{ and } \sum'_{x,y} \approx \sqrt{2}\,\sigma'_{x,y} \tag{49}$$

so Eq. (41) yields

$$B_k = \frac{\eta_k}{8\pi^2 \sigma_x \sigma_y \sigma'^2_R} = \frac{\eta_k}{8\pi^2 \varepsilon_x \varepsilon_y} \quad . \tag{50}$$

Example 2. Low-Beta Insertions:

$$\sigma'_{x,y} \gg \sigma'_R \tag{51}$$

$$\sigma'_{x,y} \frac{L}{2} \approx \sigma_{x,y} \tag{52}$$

Together, (51) and (52) imply

$$\beta^*_{x,y} \approx \frac{L}{2} \ , \tag{53}$$

$$\varepsilon_{x,y} \gg \lambda_k/2 \ . \tag{54}$$

In this case

$$\Sigma_{x,y} \approx \sqrt{2}\ \sigma_{x,y} \text{ and } \Sigma'_{x,y} \approx \sigma'_{x,y} , \tag{55}$$

hence Eq. (41) shows

$$B_k = \frac{\eta_k}{8\pi^2 \sigma_x \sigma'_x \sigma_y \sigma'_y} = \frac{\eta_k}{8\pi^2 \varepsilon_x \varepsilon_y} , \tag{56}$$

which is equal to the result for the high-beta insertion.

From Eqs. (50) and (56), we can give the following estimate of the brightness of an undulator, which should be useful for design purposes:

$$B_k = 1.8 \times 10^{12} \frac{N}{k} \frac{F_k(K)}{\varepsilon_x \varepsilon_y} \left(1 + \frac{K^2}{2}\right) , \tag{57}$$

expressed in [photons/sec, 0.1% bandwidth, $(\text{mrad})^2$, mm^2, Amp], when $\varepsilon_{x,y}$ are expressed in mm-mrad. For the first harmonic and K small (say $K \lesssim 1$),

$$B_1 \approx \frac{1.8 \times 10^{12}}{\varepsilon_x \varepsilon_y} \frac{NK^2}{1 + \frac{K^2}{2}} . \tag{58}$$

We conclude from our previous discussion that the brightness of the undulator does not depend sensitively on the value of the beta function, as long as

$$\varepsilon / \sigma'^2_R \gtrsim \beta^*_{x,y} \gtrsim \frac{L}{2} . \tag{59}$$

The key to achieving high source brightness for an undulator is to obtain small electron beam emittances. For a given machine, the emittances depend quadratically on energy, $\epsilon_{x,y} \sim \gamma^2$, so at the cost of softening the radiation the brightness can be increased by operating at lower energy.

Since the photon energy is proportional to γ^2/λ_o, the only way to obtain hard photons at smaller γ is to reduce the undulator period.[10] However, there is a practical limit on how small λ_o can be made without having K become very small. Very small K values are not desirable, since Eq. (58) shows that the brightness at ω_1 is proportional to K^2. If G is the full gap of the undulator magnet, one finds that the peak field varies as

$$B_o \sim \exp(-\pi G/\lambda_o), \tag{60}$$

so B_o becomes very small for small λ_o unless the gap G is also reduced. The minimum gap allowed by the operation of the storage ring thus limits how small λ_o can be made. A fixed gap is restricted by the requirement that at injection the vacuum chamber must be at least 2 cm high everywhere. If the gap is variable, i.e. large at injection and then narrowed after stored beam, then the minimum gap during running is limited by quantum lifetime effects, transverse resistive wall instabilities, and gas scattering. Only a test of a variable gap device will tell how small the gap can be for the NSLS, but estimates now are about 7-8 mm in the x-ray ring and 14 mm in the VUV ring. Such a test is planned with the potential of closing the gap to about 5 mm. A variable gap device will be built at the NSLS in the near future.

Let us conclude this section by recalling that the brightness is a key parameter in determining the utility of a source for holography. If the source size is characterized by $\sum_{x,y}$ then only the radiation within a solid angle

$$\Delta\Omega \approx \frac{\lambda^2}{4\sum_x \sum_y} \tag{61}$$

is spatially coherent.[11] From Eq. (40), we see that the coherent flux[11] within this solid angle is

$$\eta_c \approx B(\lambda)\lambda^2 , \tag{62}$$

showing the importance of high brightness $B(\lambda)$ and the difficulty of holography at short wavelengths. Undulators hold promise as sources for x-ray holography.

IV. X-RAY DEVICES UNDER CONSTRUCTION

Having presented an outline of the basic concepts underlying the use of wigglers and undulators, we will now discuss the insertion devices currently under construction for the NSLS facility, and in later sections we also discuss several magnets which could be constructed in the near future. We emphasize the spectral properties of the radiation produced by the different devices, and we shall consider some limitations posed by the energies of the storage rings, vertical beam aperture, and emittance.

There are two wigglers now under construction for the x-ray ring, whose specific properties are quite different and are summarized in Tables 4.1 and 4.2. The first device which we will discuss is the superconducting wiggler. From Table 4.1 it is seen that this is a $2N = 6$ pole, $B = 6$ T superconducting magnet with a period length of 17.4 cm. The K value of 97 identifies it as a true wiggler with a continuous synchrotron radiation spectrum. Of course, the most important feature of the superconducting wiggler spectrum is the shift of the critical wavelength to about $\lambda_c = 0.5$ Å. The effective 6 poles also give a factor of 6 in intensity at longer wavelengths. A comparison of the superconducting wiggler spectrum with the arc source is given in Fig. 4.1.

In Table 4.1 the effective horizontal $\Delta\theta_{1/2} = 12$ mrad is calculated assuming only a 20% variation from the peak field (See Sect. II, Eq. (21) and the discussion there). In fact, the vacuum chamber walls will restrict the horizontal radiation taken out of the beam port to about 12 mrad total.

The superconducting wiggler will radiate a large amount of power. For operation at 0.5 A and 2.5 GeV the integrated power will be ~ 1 kW/mrad horiz., a total of ~ 37 kW. Such a high power level may be difficult to deal with on the optics, but at the NSLS there is no other way to get the high energy photons. In fact Fig. 4.1 shows that there will be considerable flux up to about 100 keV.

Another wiggler for the x-ray ring is the vanadium permandur-rare earth cobalt (REC) hybrid wiggler summarized in Table 4.2. This is a permanent magnet structure consisting of blocks of $SmCo_5$ (permanent magnets) and high μ poles of either vanadium permandur or mild steel placed at strategic locations. The design is due to K. Halbach[12] and researchers at the High Energy Institute in Novosibirsk,[12] and is called a "hybrid" structure, because although it is a permanent magnet, the magnetic field is shaped by the use of high μ poles as is usually done for electromagnets. The use of these poles concentrates the flux and enables one to achieve higher magnetic field strengths than are possible with permanent magnets alone. The magnet being constructed has a design value of 1.5 T for the peak field, and has $2N = 24$ poles, $\lambda_w = 13.6$ cm and a full gap of 2.0 cm. The K value is 19, and the critical wavelength is slightly shifted to shorter wavelength relative to the bending magnet, i.e. to $\lambda_c \approx 2.0$ Å. The spectrum is a continuous synchrotron radiation spectrum, but with an enhancement of a factor of 24 in integrated flux per horizontal mrad compared to the arc source. Fig. 4.1 shows the comparison clearly. This device produces a very high flux over the wavelength range covered by the bending magnets and also collimates the beam into $2\theta_{1/2}$(Effective) = 4.6 mrad. It does not harden the spectrum substantially. Its main use then

will be for very high flux in the neighborhood of 0.5 - 10 Å, but with quite high total power radiated. The total power will be 7.1 kW into 7.8 mrad.

Because of the simplicity of a permanent magnet device, it may be that the hybrid wiggler will be installed on the x-ray ring earlier than the superconducting wiggler. Therefore, it will provide an early enhanced source of hard photons at the NSLS. Also, its construction provides valuable experience, which will facilitate the construction of the undulator structures to be built in the near future (and discussed in the following sections).

Section IV. X-Ray Devices Under Construction - Tables and Figures

Table 4.1. Parameters for the NSLS Superconducting Wiggler

Maximum Field	6 Tesla
$\lambda_c(\varepsilon_c)$	0.5 Å (24.9 keV)
Number of Poles	5 (at 6 T) + 2 (at 3 T)
Period Length, λ_w	17.42 cm
Full Gap (Magnetic)	3.2 cm
Full Gap (Beam Stay Clear)	2.0 cm
Wiggler Length	1.4 m
$K = 0.93\ \lambda_w B_o$	97
$\Delta\psi_{1/2}$ (Vertical)=$(1/2\gamma)$	0.1 mrad
$\Delta\theta_{1/2}$ (Horizontal, Effective) $(=0.6\ K/\gamma)$	12 mrad
Beam Parameters	σ_x = 0.35 mm
	σ_x' = 0.25 mrad
	σ_z = 0.02 mm
	σ_z' = 0.05 mrad
Spectrum	Continuum
$N_{flux}(\lambda=\lambda_c)(I=0.5\ A)(All\ \psi)$ =	1×10^{15}(Photons/sec/mrad/1% $\Delta\lambda/\lambda$)

Table 4.2. Parameters for the Vanadium Permandur REC Hybrid Wiggler

Maximum Field	15 kG
$\lambda_c(\varepsilon c)$	2.0 Å (6.2 keV)
Number of Poles	24
Period Length, λ_w	13.6 cm
Full Gap (Magnetic)	2.0 cm
Full Gap (Beam Stay Clear)	1.8 cm
Wiggler Length	1.6 m
$K = 0.93\ \lambda_w B_o$	19
$\Delta\psi_{1/2}$ (Vertical)=$(1/2\gamma)$	0.1 mrad
$\Delta\theta_{1/2}$ (Horizontal, Effective) $(=0.6\ K/\gamma)$	2.3 mrad
Beam Parameters	σ_x = 0.35 mm
	σ_x' = 0.25 mrad
	σ_z = 0.02 mm
	σ_z' = 0.05 mrad
Spectrum	Continuum

$N_{flux}(\lambda=\lambda_c)(I=0.5\ A)(All\ \psi) = 4.8 \times 10^{15}$(Photons/sec/mrad/1% $\Delta\lambda/\lambda$)

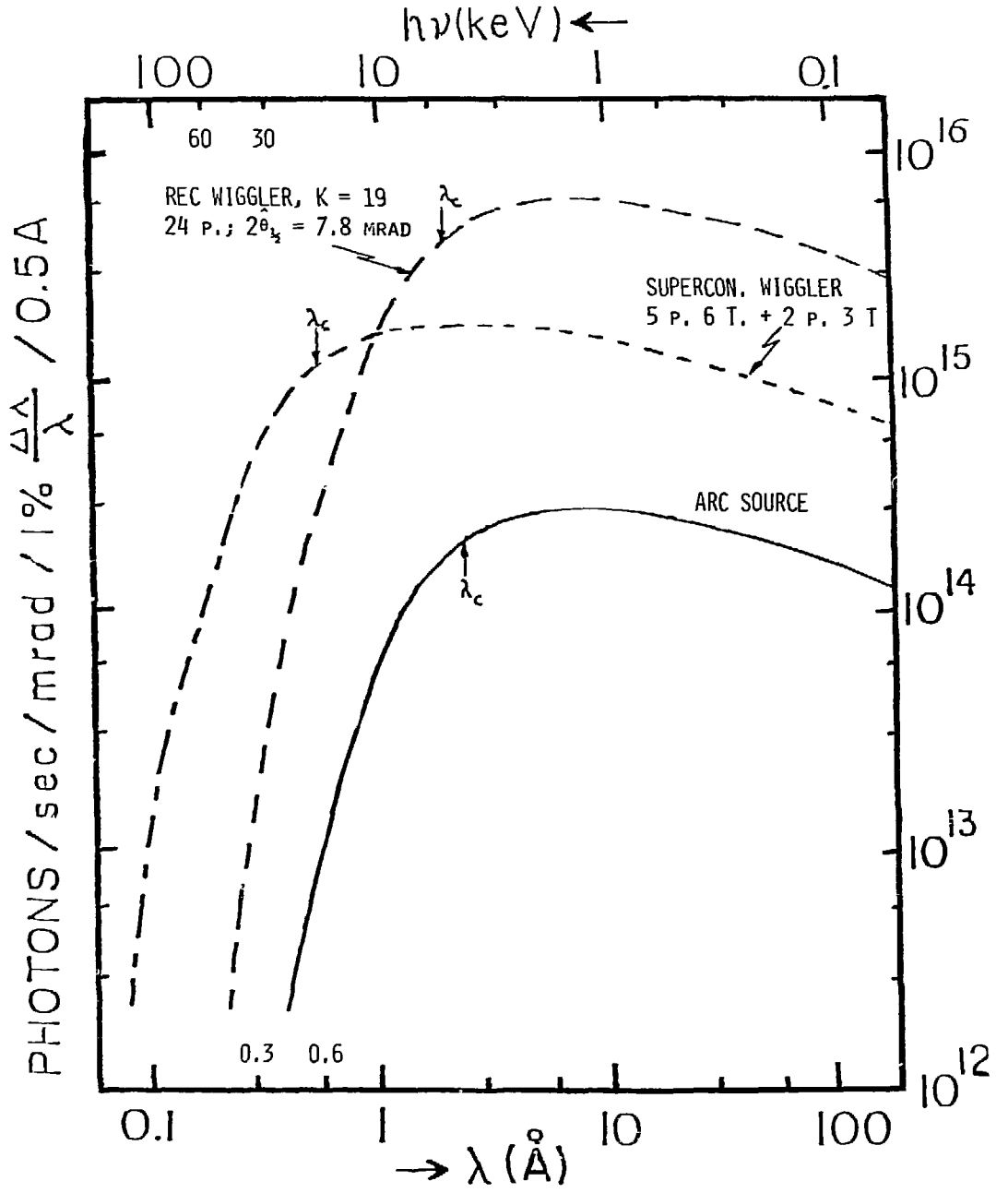

NSLS SR SPECTRA, X-RAY RING, 2.5 GeV

Fig. 4.1

V. VUV DEVICES UNDER CONSTRUCTION

An experiment[13] designed to study the operation of a free electron laser (FEL) in a storage ring is underway at the NSLS. A permanent magnet[14] REC ($SmCo_5$) undulator has been constructed for this experiment and will be installed on the VUV ring early this fall. Some of the important parameters of this undulator are presented in Table 5.1. The structure has 38 periods with the period length λ_o = 6.5 cm. The magnet gap can be varied from 1-6 cm corresponding to K values from 4.3-0.4. For example, when the gap is 2 cm, then K = 2.4. The FEL experiment requires a large value of K ≈ 3.3, in order to produce a fundamental wavelength of 3500 Å at an electron energy of 380 MeV.

The FEL undulator will be made available to experimenters interested in using this enhanced source for synchrotron radiation research. In Fig. 5.1, we show the spectrum for K = 1 of the radiation emitted into a cone about the forward direction of half-angle $\theta = 0.5/\gamma = 0.36$ mrad. The fundamental is located at 260 Å, and has a peak photon flux of 3×10^{16} (photons/sec, 1% bandwidth, Ampere). In Fig. 5.2 we show the spectrum for K = 1.4 integrated over all angles. The fundamental is softened to 346 Å, and the peak flux is 4.5×10^{16} (photons/sec, 1% bandwidth, Ampere). The third harmonic peak located at 115 Å has a peak flux of 2×10^{16} (photons/sec, 1% bandwidth, Ampere). By tuning the field strength parameter in the range $0.5 \leq K \leq 2.5$, high flux can be obtained in the wavelength range 80 - 500 Å.

An interesting exercise is to consider the results of putting the REC hybrid wiggler (Sect. IV) on the UV ring. The spectrum integrated for $2\theta_{1/2}$ = 10 mrad is shown in Fig. 5.3 and is compared with the angle integrated flux for both the arc source ($2\theta_{1/2}$ = 10 mrad) and the FEL undulator operating at K = 2.4, ($2\theta_{1/2}$ = 3.5 mrad). The factor of 2N intensity increase relative to the arc source is clear. By chance the flux is about the same as the FEL undulator in the wavelength range $\lambda > 100$ Å. In the range where the fluxes are comparable the undulator would be the device of choice, because of its intrinsic brightness. It does not suffer as much from source broadening, $2\sum_x \sim L\theta$, for an angle of observation θ. The total power radiated by the K = 2.4 undulator is also a factor of 0.11 less than the wiggler (Eq. 24).

Section V. VUV Devices Under Construction - Tables and Figures

Table 5.1. Parameters for the FEL undulator used on the VUV ring for the free electron laser experiment.

Fig. 5.1 The spectrum of the radiation from the FEL undulator with $K = 1$, $\gamma = 1370$, radiated into a cone about the forward direction of half-angle $\theta = 0.5\ \gamma = 0.36$ mrad.

Fig. 5.2 The angle integrated spectrum from the FEL undulator with $K = 1.4$, $\gamma = 1370$.

Fig. 5.3 A comparison of the angle integrated flux from the NSLS VUV bending magnets with that for a) the NSLS REC wiggler operating on the VUV ring with $K = 19$ and $2\theta_{1/2} = 10$ mrad and b) the VUV undulator operating at $K = 2.4$.

Table 5.1. Parameters for the FEL Undulator Used on the VUV Ring for the Free Electron Laser Experiment

Structure	$SmCo_5$
Number of Periods	38
Period Length	6.5 cm
Full Gap (Magn. = Stay Clear)	1-6 cm
Undulator Length	2.5 m
Deflection Parameter (K)	4.3 - 0.4
Gap	2.0 cm (K = 2.4)
$2\theta_{1/2}$	3.5 mrad
Beam Parameters	σ_x = 1.0 mm
	σ_x' = 0.09 mrad
	σ_z = 0.08 mm
	σ_z' = 0.01 mrad
Spectrum	Figures 5.1, 5.2

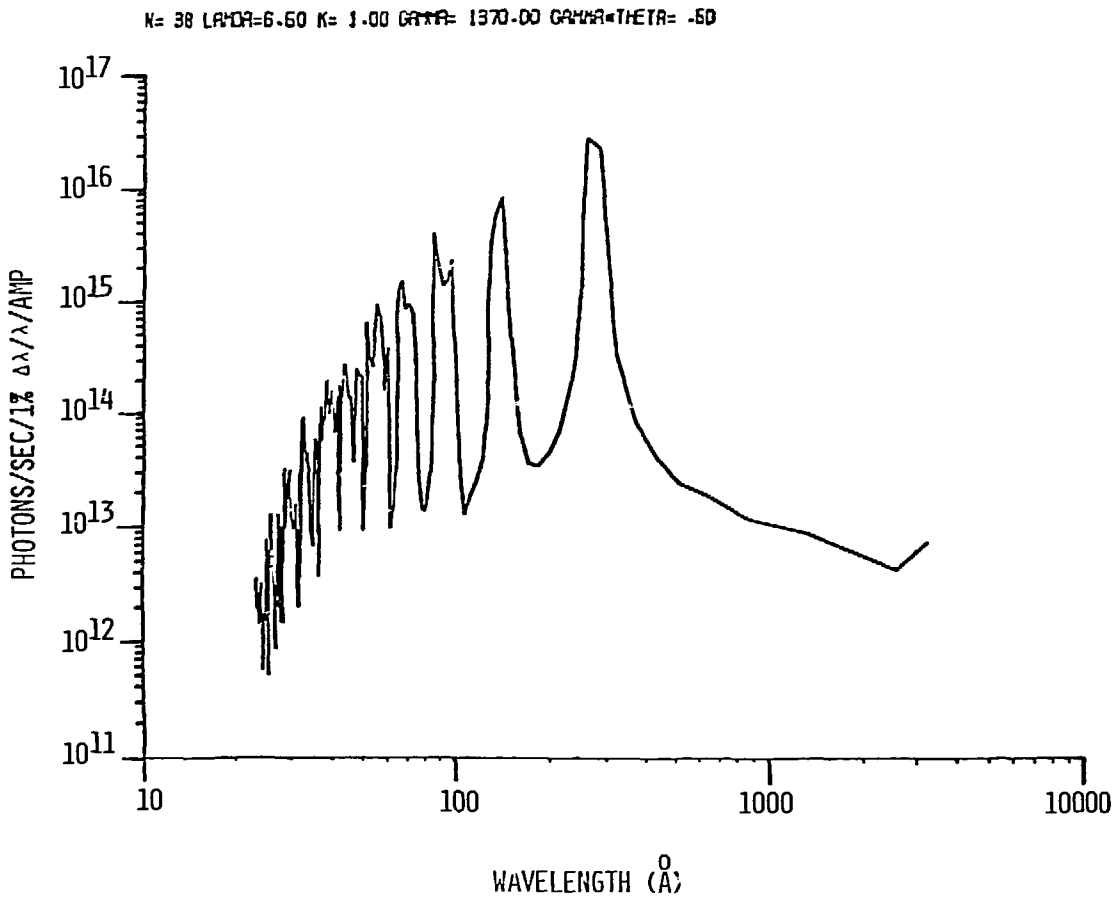

NSLS UNDULATOR (K = 1) SPECTRUM, VUV RING

Fig. 5.1

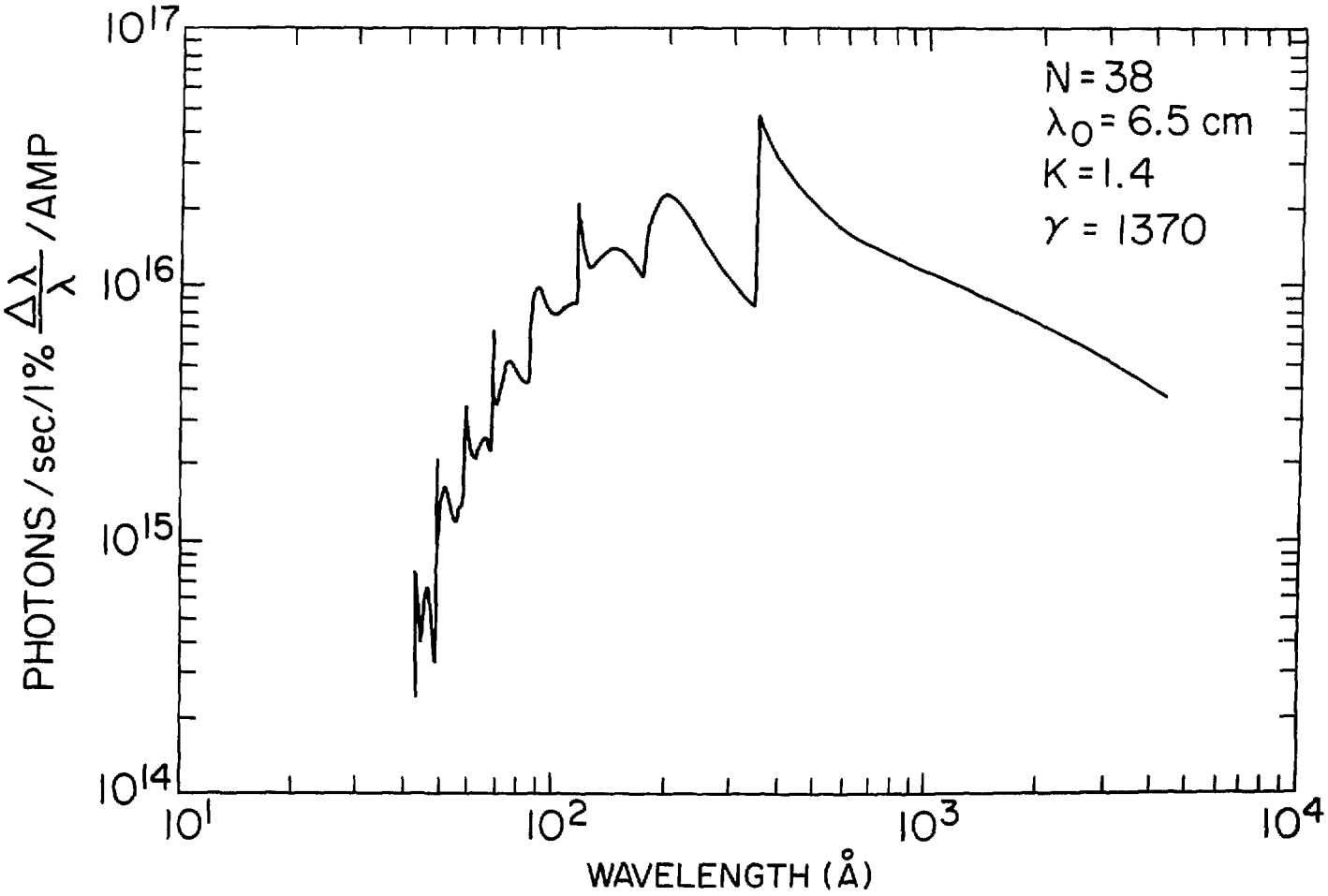
N = 38
λ0 = 6.5 cm
K = 1.4
γ = 1370
PHOTONS / sec / 1% Δλ/λ / AMP
WAVELENGTH (Å)
10^17
10^16
10^15
10^14
10^1
10^2
10^3
10^4

Fig. 5.2

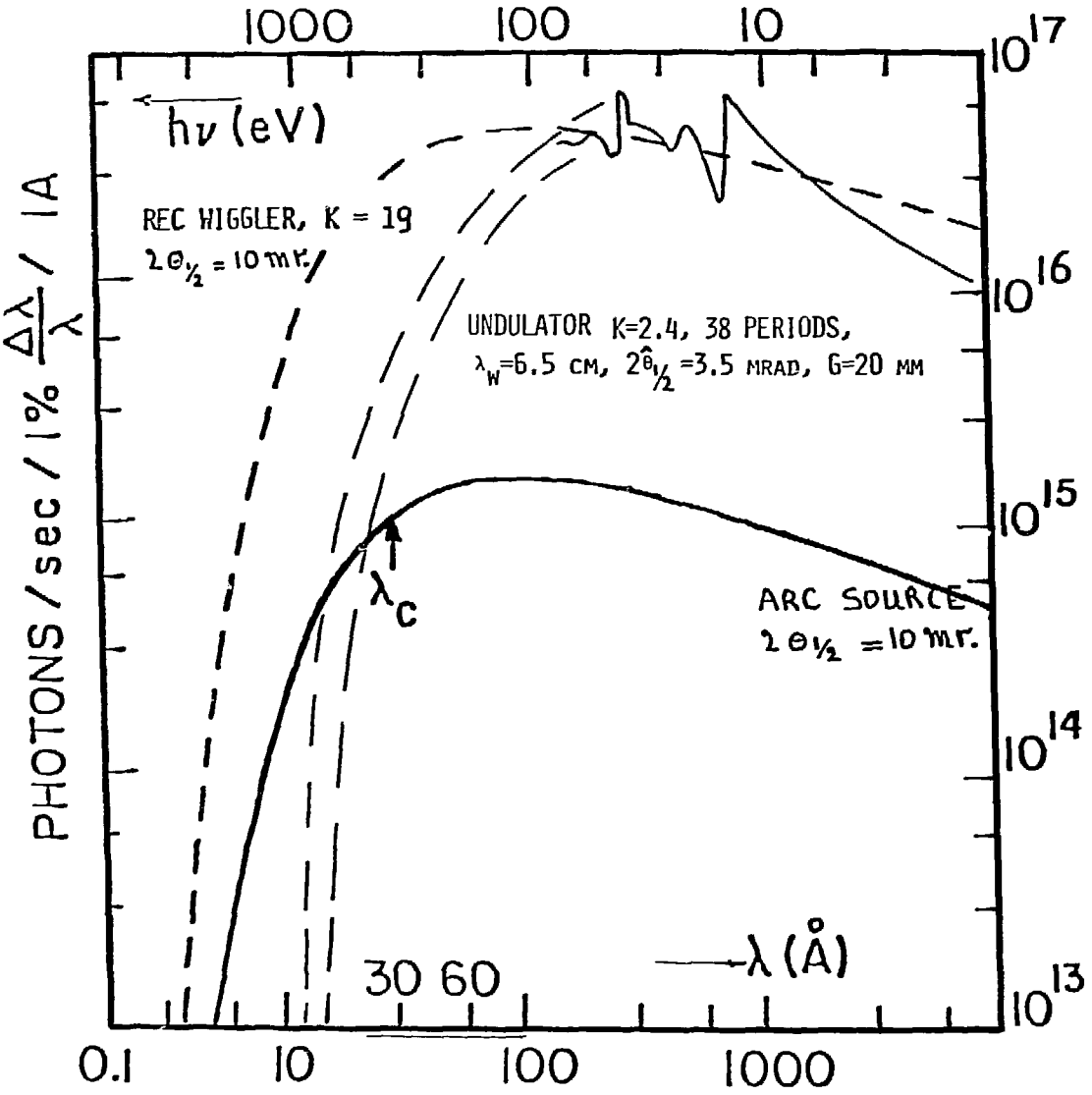

NSLS SPECTRUM, VUV, 0.7 GeV

Fig. 5.3

VI. POSSIBLE X-RAY UNDULATORS

The next generation of insertion magnets for the NSLS (primarily the x-ray ring) will have to be designed in close collaboration with the experimental programs which will use the radiation. This is necessary because the spectra in general will be from undulators, due to their high flux, extreme brightness, and low-total power. Since the undulator fundamental and harmonic frequencies are determined by the design, the choice must be made early. Of course, the NSLS will learn much in the next year or two concerning the minimum gap and hence minimum wavelengths achievable. In this section we shall discuss two classes of devices which we are confident can be built: (A) Soft X-ray Undulators (SXU) with $5 < \lambda < 50$ Å, and (B) High Energy Undulators (HEU) with $3 < \lambda < 12$ Å.

A. Soft X-Ray Undulators (SXU)

The primary intent of these devices would be to produce high intensity, highly collimated radiation in the 5–50 Å range. We will discuss two operating modes, one which produces a reasonably continuous spectrum, and one which produces the true undulator spectrum of discrete harmonics.

Table 6.1 lists a set of typical parameters for a hybrid vanadium permandur - S_mCo_5 SXU. Let us consider first a K = 3, 40 period (80 pole) device with λ_o = 6 cm. The spectrum will be as shown in Fig. 6.1. For $\lambda < 50$ Å the spectrum (angle integrated) shows a basic synchrotron radiation dependence, except that it has a ripple due to the undulator

harmonics superimposed on it. The flux is very intense and collimated into $2\theta_{1/2}$ = 1.2 mrad. For experiments in which the ripple would not pose a problem this would be a bright source of moderate power. Note that the ripple is expected to decrease as the K value of a device increases. As stated earlier, the spectrum for $K \gg 1$ no longer is that of an undulator, but becomes a synchrotron radiation spectrum characterized by a critical frequency $\omega_c = k_c \omega_1$, with $k_c = 3/8\ K^3$. At ω_c many harmonics contribute (on the order of k_c harmonics) to the spectrum and we may expect that the resulting ripple will be only on the order of

$$\Delta\eta/\eta \sim k_c^{-1} \sim K^{-3}.$$

The spectrum for another device for the x-ray ring with K = 3, λ_u = 6 cm, but with fewer poles (48) is shown in Fig. 6.2. The spectrum (photons/sec/mrad/1% $\Delta\lambda/\lambda$/.5 Amp) is shown smoothed with the fundamental at about 70 Å. We also compare this spectrum in Fig. 6.2 with the angle integrated spectra obtained from the superconducting wiggler ($2\theta_{1/2}$ = 5 mrad), REC wiggler ($2\theta_{1/2}$ = 5 mrad), and the arc source ($2\theta_{1/2}$ = 5 mrad). The advantages of the K = 3 undulator relative to the arc source are its high intensity and brightness ($2\theta_{1/2}$ = 1.2 mrad) in the range $5 < \lambda < 50$ Å, and low power, 810 W (675 W/mrad). At wavelengths less than 5 Å the K = 3 undulator is not competitive with the wigglers in flux.

To take full advantage of the properties of an undulator one would not operate the device in the manner just described. Instead a device would be

designed with a low K value, many periods, and a fundamental in the range of interest. Figures 6.3 and 6.4 show the integrated flux for an N = 35, λ_o = 6 cm device for which K = 1.4 and 0.5, respectively. Each of these will collimate the radiation very highly with $2\theta_{1/2}$ = 0.6 mrad for K = 1.4 and $2\theta_{1/2}$ = 0.2 mrad for K = 0.5. These spectra have the fundamental occurring at energies of 0.4 and 0.8 keV, with very high flux, 10^{16} - 10^{17} (photons/sec/1% $\Delta\lambda/\lambda$/Amp). The radiated power is quite low being only about 32 W into the 0.4 mrad for the K = 0.5 device.

The characteristic broadening of the peaks on the low energy side is clearly illustrated in Figs. 6.3 and 6.4. Due to the angular dependence of the spectrum noted in Eq. 9, the spectrum softens at higher observation angles giving a sharp edge on the high energy side and the long low-energy tail. Some tuning of these peaks could occur for a variable gap magnetic device. It seems clear that one would chose one of these devices for many experiments tuned to a specific wavelength, instead of one of the K = 3 undulators discussed above since the radiation is of equal intensity but with more collimation and less radiated power.

VI. A. Possible Soft X-Ray Devices ($5 < \lambda < 50$ Å) - Tables and Figures

Table 6.1 Parameters for a permanent magnet soft x-ray undulator (SXU) for the NSLS X-ray ring (N = 40, λ_o = 6 cm, K = 0.5-3).

Fig. 6.1 Angle integrated flux for the soft x-ray undulator (SXU) operating on the x-ray ring with K = 3, N = 40, λ_o = 6 cm.

Fig. 6.2 A comparison with the flux from the NSLS x-ray bending magnets of the integrated flux from several devices:

a. The superconducting wiggler ($2\theta_{1/2}$ = 5 mrad)

b. The REC wiggler, K = 19 ($2\theta_{1/2}$ = 5 mrad)

c. The 48 period REC soft x-ray undulator operating at K = 3 ($2\theta_{1/2}$ = 1.2 mrad)

The $2\theta_{1/2}$ values for the two wigglers are the 5 mrad horizontal values used for the integration.

Fig. 6.3 The angle integrated spectrum for a soft x-ray undulator on the x-ray ring. The parameters for this device are K = 1.4, N = 35, λ_o = 6 cm.

Fig. 6.4 The spectrum for the first harmonic of the same device as in Fig. 6.3, except that the gap has been chosen to allow operation at K = 0.5.

Table 6.1. Parameters for a Permanent Magnet Soft X-Ray Undulator (SXU) for the NSLS X-ray Ring (N = 40, λ_o = 6 cm, K = 0.5-3)

Structure	VP-$SmCo_5$
Number of Periods	40
Period Length λ_w	6.0 cm
Full Gap (Magn. = Stay Clear)	5-25 mm, variable
Full Gap, Operational Objective	10 mm
Undulator Length	2.5 m
Deflection Parameter (K)	0.5 - 3.0
Gap	10-20 mm
$2\Delta\theta_{1/2}$	2.0-1.2 mrad
Beam Parameters	σ_x = 0.35 mm
	σ_x' = 0.25 mrad
	σ_z = 0.02 mm
	σ_z' = 0.05 mrad
Spectrum	Figures 6.1-6.4
N_{flux} (I=0.5Å)(all ψ)(photons/sec/1% $\Delta\lambda/\lambda$)	$5 \cdot 10^{16}$-$2 \cdot 10^{16}$

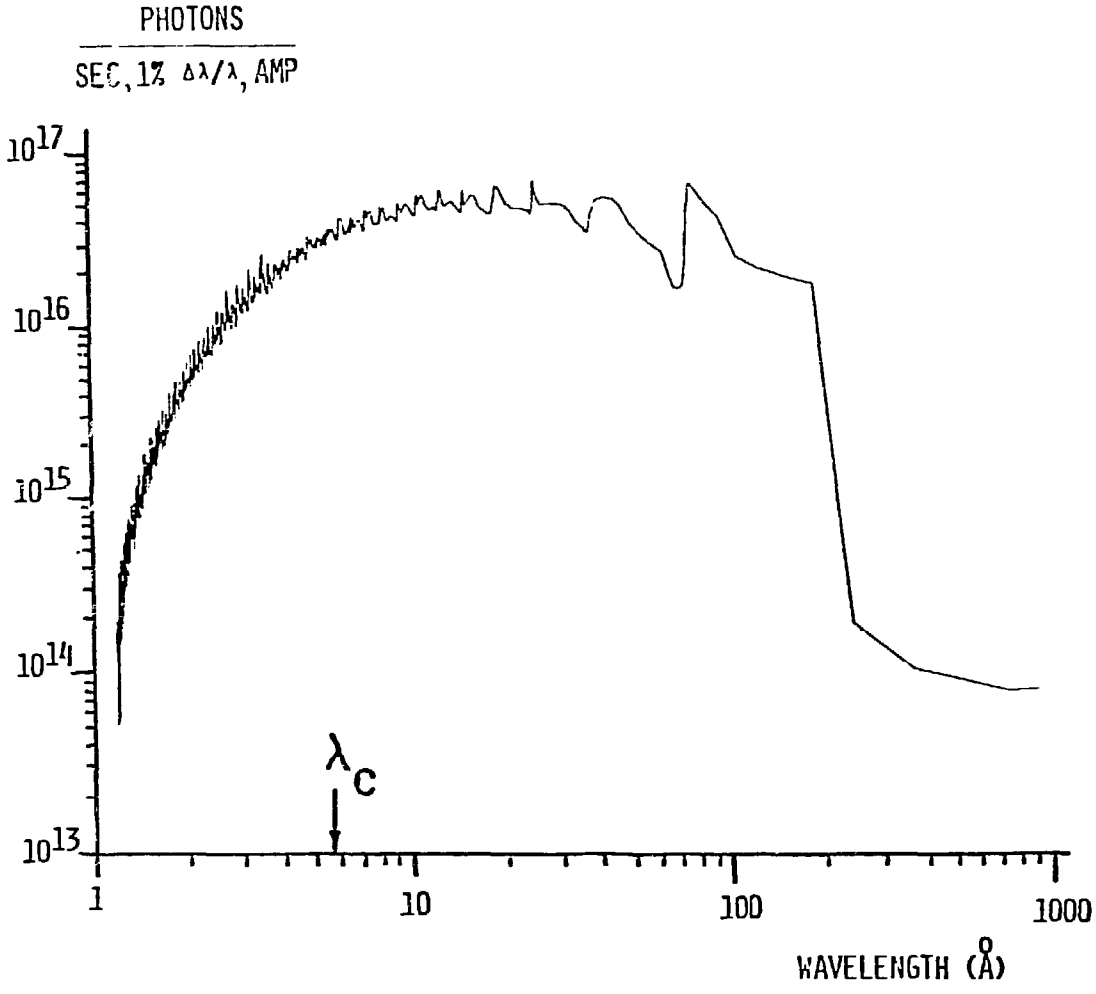

NSLS UNDULATOR SPECTRUM, X-RAY, 2.5 GeV

(K = 3, 40 PERIODS, λ_W = 6 CM, $2\hat{\theta}_{\frac{1}{2}}$ = 1.2 MRAD, G = 20 MM, $\gamma\theta$ = 3.0)

Fig. 6.1

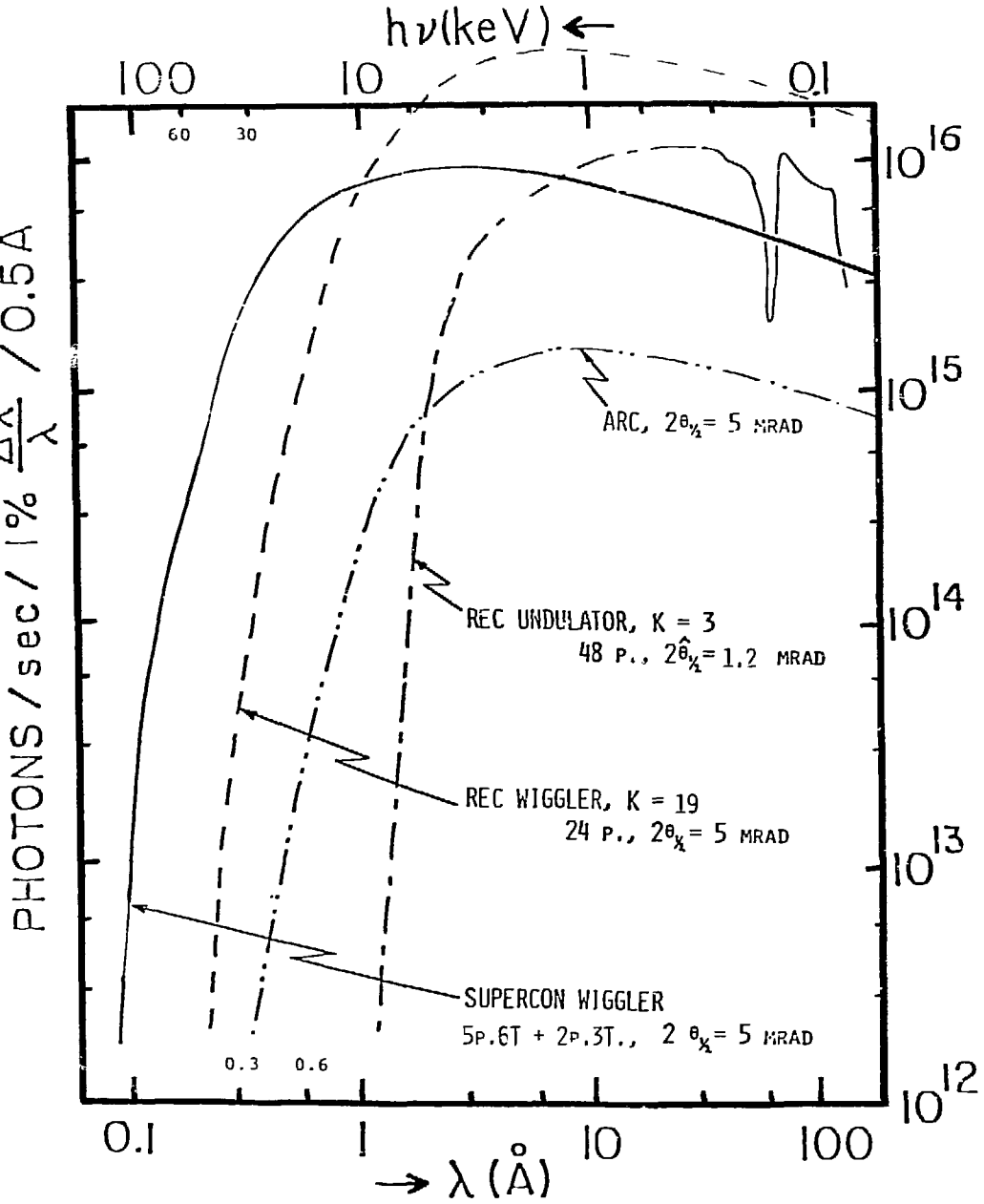

NSLS, SPECIAL SOURCES, X-RAY RING, 2.5 GeV

Fig. 6.2

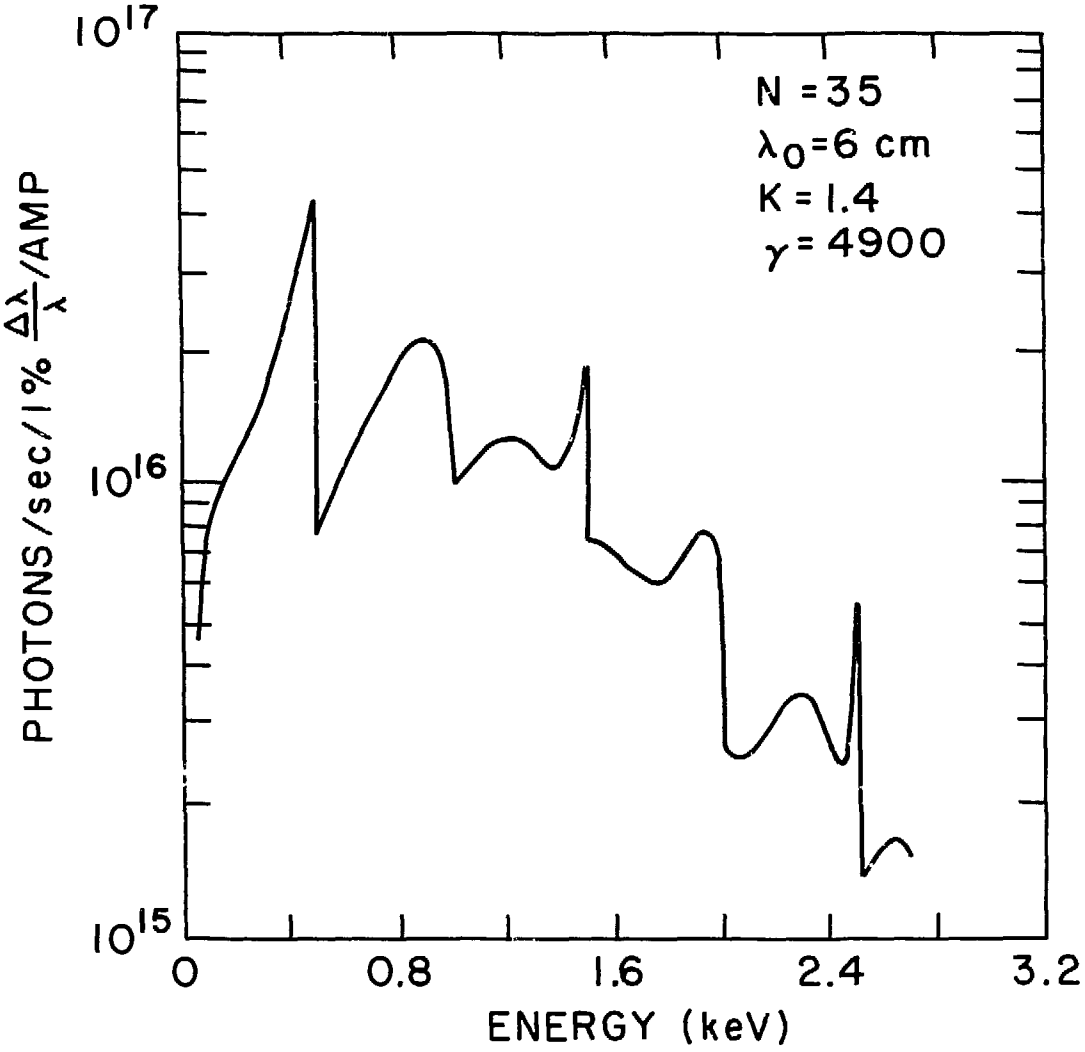
10^{17}
10^{16}
10^{15}
PHOTONS/sec/1% $\frac{\Delta\lambda}{\lambda}$/AMP
N = 35
λ_0=6 cm
K = 1.4
γ = 4900
0
0.8
1.6
2.4
3.2
ENERGY (keV)

Fig. 6.3

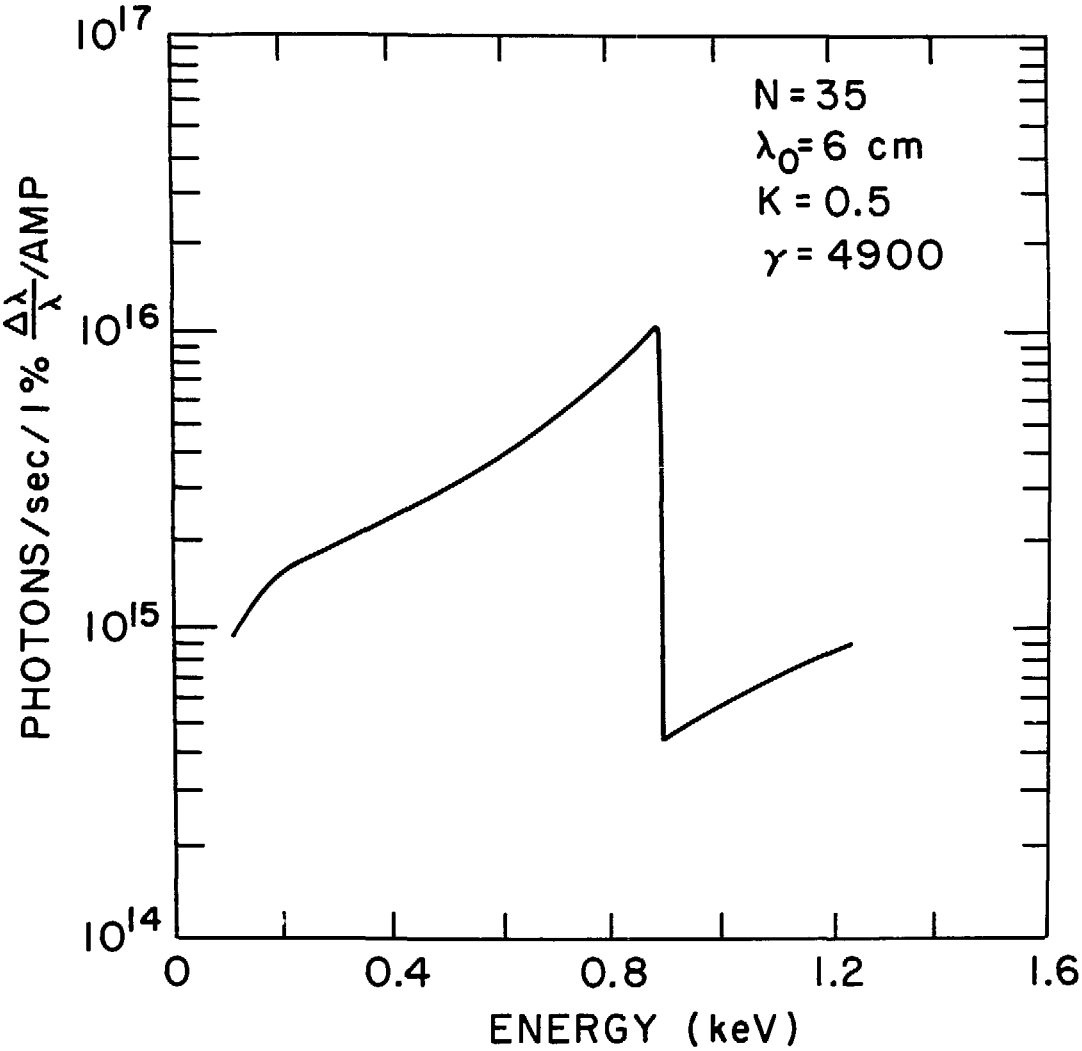
N = 35
λ_0 = 6 cm
K = 0.5
γ = 4900
10^{17}
10^{16}
10^{15}
10^{14}
PHOTONS/sec/1% $\frac{\Delta\lambda}{\lambda}$/AMP
0
0.4
0.8
1.2
1.6
ENERGY (keV)

Fig. 6.4

B. High Energy Undulators (HEU)

Ultimately the desire is to produce undulators which have fundamentals in the hard x-ray range. But, as stated earlier, the gap closure will limit the energy obtainable. If the gap can be closed to as small as 7 mm, however, one can imagine devices with a fundamental as high as about 3.5 keV. Table 6.2 includes the parameters for a high energy undulator (HEU) with a set of possible values for K and the gap. Figures 6.5 and 6.6 show the angle integrated spectra for an N = 100, λ_o = 2.2 cm device with K = 1.0 and 0.5, respectively. These values of K correspond to gaps of about 7-11 mm and photon energies of 1.9 and 2.4 keV at the first harmonic peak. From Fig. 6.5 we see that the third harmonic peak corresponds to a flux of 2 x 10^{16} (photons/sec, 1% bandwidth, Ampere) at a photon energy of 5 keV.

The HEU's are very bright sources with $2\theta_{1/2} \sim \gamma^{-1}$ and very high intensities. Quantitative comparisons in terms of flux and source brightness for a few specific x-ray undulators and wigglers cited in this report are given elsewhere.[15] The extreme brightness, as highlighted earlier, means a very high efficiency in useful photons/unit power radiated and a corresponding ability to deliver high photon flux to a sample with extremely small source size and/or angular acceptance aberrations. The optics for such experiments as crystallography on small samples and for microprobe analysis become reasonably straightforward. The problem to be faced, however, will be the handling of the high power densities from these sources.

One final comparison of devices is useful to highlight some of the ideas presented. Fig. 6.7 shows a soft x-ray undulator (slightly different parameters than that shown in Fig. 6.2) with K = 3, N = 33, and λ_u = 6 cm compared to a high energy undulator with K = 1.4 and K = 0.5. The HEU is

also slightly different than that shown in Figs. 6.5 and 6.6, since it has N = 67 and λ_u = 3 cm. It is clear that for $\lambda > 20$ Å the SXU has an order of magnitude more flux. But, for $\lambda < 20$ Å the HEU for K = 1.4 gives comparable flux and is a brighter source ($2\theta_{1/2}$ = 0.57 mrad) with comparable radiated power. If an experimental program demands the optimized radiation source in the $6 < \lambda < 20$ Å wavelength range, then the HEU with K = 0.5 would be the choice. It has the same flux as the other two devices, but is collimated into $2\theta_{1/2}$ = 0.2 mrad and this is a factor of 6 brighter than the SXU, and a factor of 3 brighter than the HEU at K = 1.4. The K = 0.5 HEU will radiate only 120 W of total power compared to about 1 kW for the other devices. Thus, it is essential to know the dominant wavelength range in which experiments will be done in order to specifically design the optimized sources.

VI. B. Possible High Energy Undulators ($2 < \lambda < 12$ Å) - Tables and Figures

Table 6.2 Parameters for a permanent magnet high energy undulator (HEU) for the NSLS x-ray ring (N = 100, λ_o = 2.2 cm, K = 0.5-1.0)

Fig. 6.5 Angle integrated flux for an x-ray undulator with N = 100, λ_o = 2.2 cm, and K = 1. The value of the gap is 6-7 mm.

Fig. 6.6 The same device as Fig. 6.5 except with K = 0.5.

Fig. 6.7 A comparison of a soft x-ray undulator (K = 3, λ = 6 cm, N = 33) with a high energy undulator operating with K = 0.5 and K = 1.4.

Table 6.2. Parameters for a Permanent Magnet High Energy Undulator (HEU) for the NSLS X-ray Ring (N = 100, λ_o = 2.2 cm, K = 1-0.5)

Structure	VP-$SmCo_5$ Hybrid
Number of Periods	100
Period Length λ_w	2.2 cm
Full Gap (Magn. = Stay Clear)	5-25 mm, variable
Full Gap, Operational Objective	7 mm
Undulator Length	2.5 m
Deflection Parameter (K)	1-0.5
Gap	10-20 mm
$2\Delta\theta_{1/2}$	0.7-0.25 mrad
Beam Parameters	σ_x = 0.35 mm
	σ_x' = 0.25 mrad
	σ_z = 0.02 mm
	σ_z' = 0.05 mrad
Spectrum	Figures 6.5-6.7
N_{flux} (I=0.5Å)(all ψ)(photons/sec/1% $\Delta\lambda/\lambda$)	$5 \cdot 10^{16}$-$1 \cdot 10^{16}$

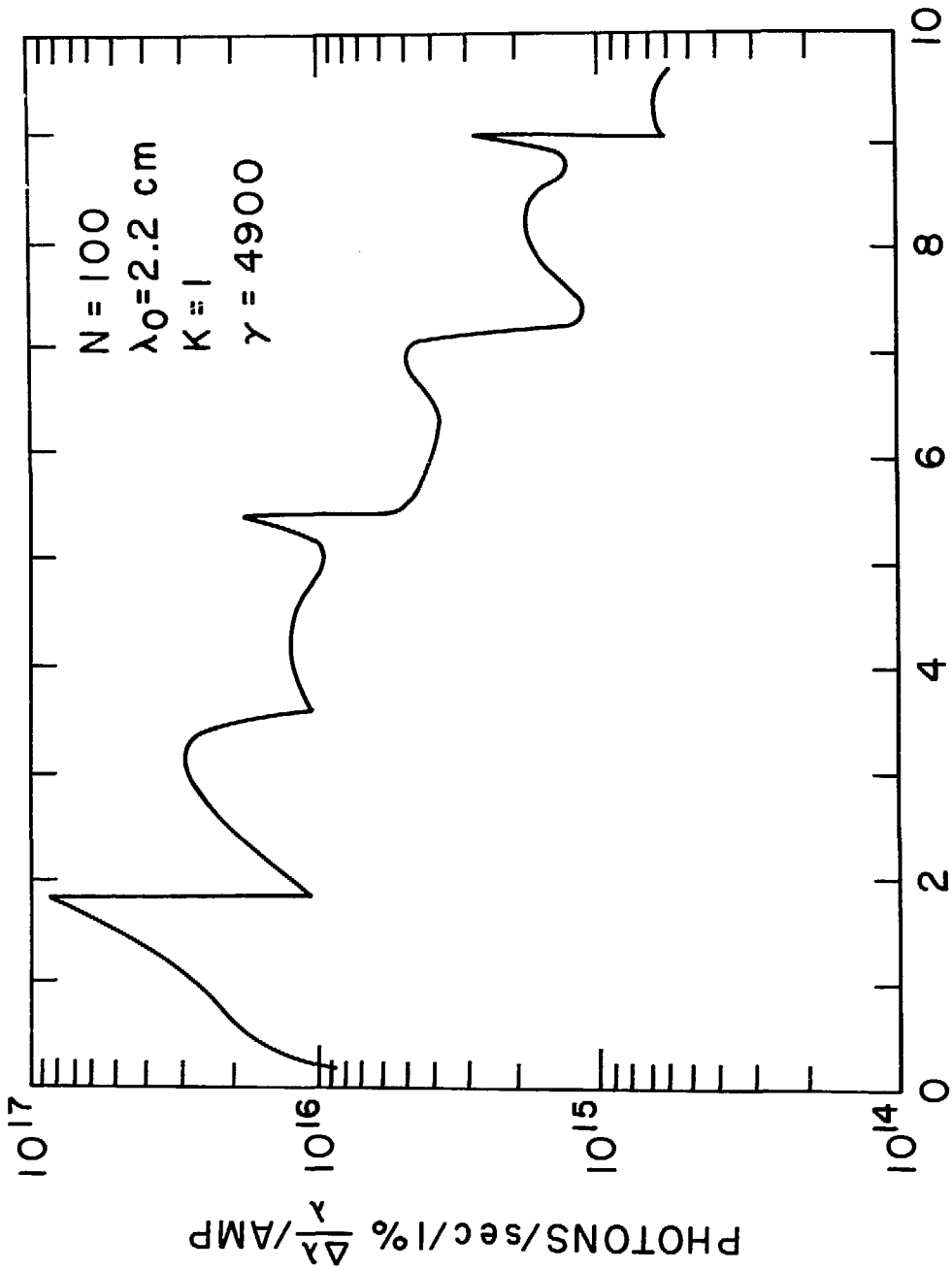
N = 100
λo=2.2 cm
K = 1
γ = 4900
PHOTONS/sec/1% Δλ/λ/AMP
ENERGY (keV)
10^17
10^16
10^15
10^14
0
2
4
6
8
10

Fig. 6.5

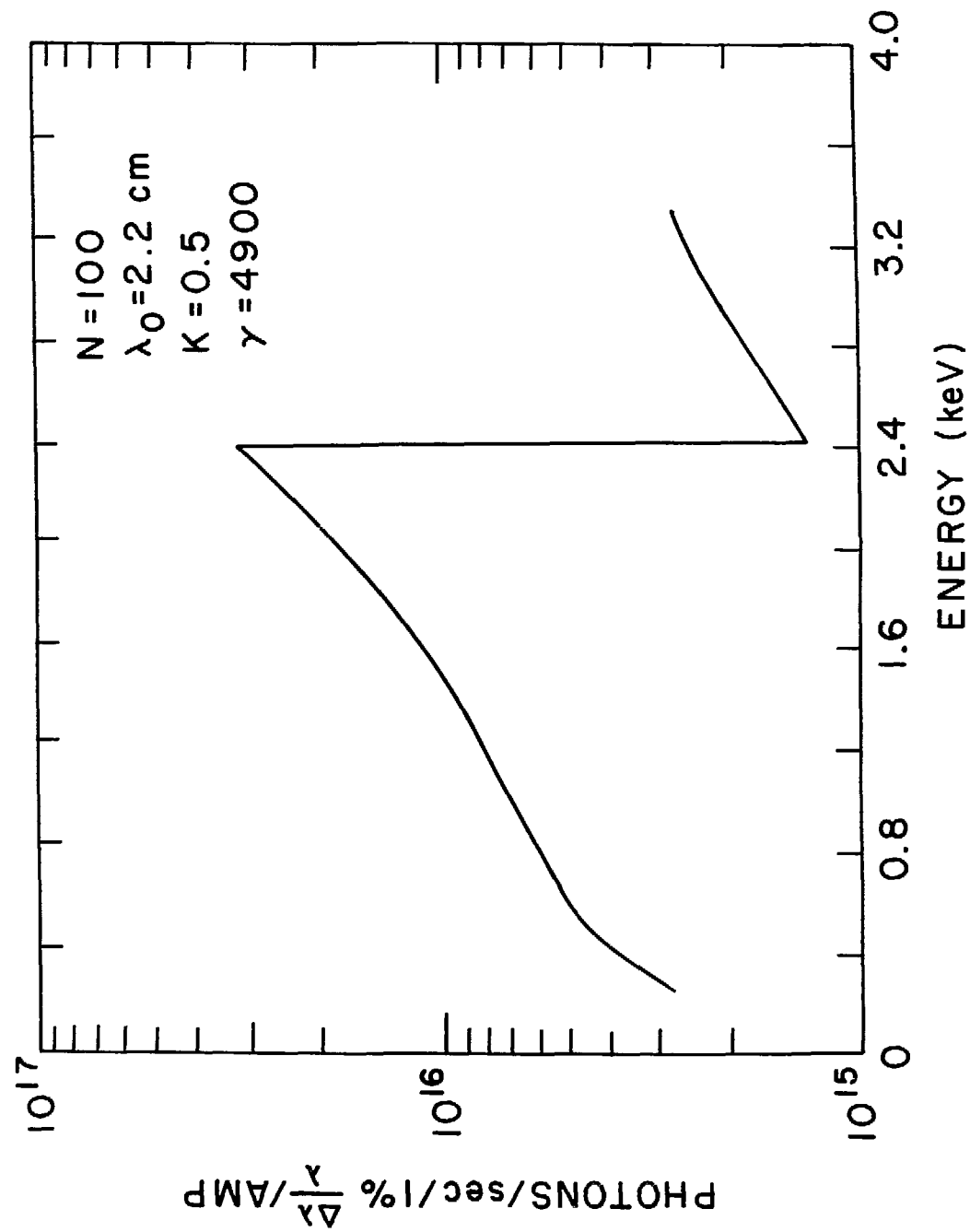
N=100
λ_0=2.2 cm
K=0.5
γ=4900
10^{17}
10^{16}
10^{15}
PHOTONS/sec/1% $\frac{\Delta\lambda}{\lambda}$/AMP
0
0.8
1.6
2.4
3.2
4.0
ENERGY (keV)

Fig. 6.6

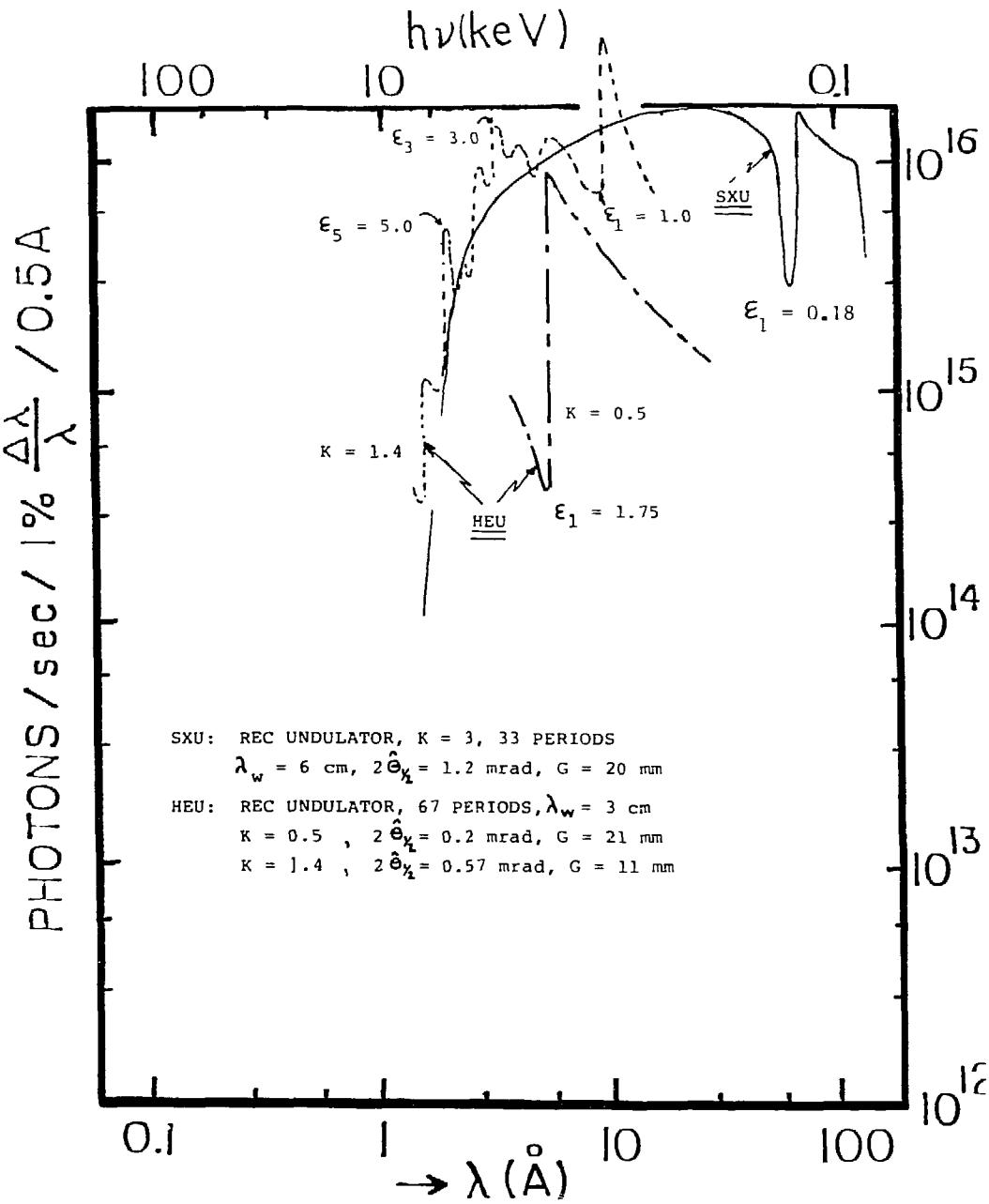

NSLS, SPECIAL SOURCES, X-RAY RING, 2.5 GeV

Fig. 6.7

VII. CONCLUDING REMARKS

An undulator ($K \lesssim 1$) yields a high photon flux with a small total radiated power. Additional enhancement of flux per steradian results when the angular spread of the electron beam passing through the undulator is sufficiently small. This condition is satisfied now on the VUV ring, but one would need high-beta insertions on the x-ray ring. As discussed in Section III, because the source size is increased, there is no gain in brightness in going to high-beta. The regime of $K \approx 2\text{-}5$ can yield enhancement of hard photon flux per steradian, but there may be a troublesome ripple. For $K > 10$, the spectrum in the neighborhood of the critical wavelength is well approximated by 2N times the synchrotron radiation spectrum, but we must recall that the effective source size becomes large upon accepting a large angular bite, $\Sigma_x \sim L\theta/2$. The enhancement of the photon flux at wavelengths less than about 2 Å at the NSLS requires high field wigglers. At the operating energy of 2.5 GeV the very short magnetic period length needed to produce hard photons from an undulator require very small magnet gaps to generate reasonable field strengths. The magnet gap cannot be made arbitrarily small, because of the necessary stay-clear aperture of the stored electron beam.

The discussion presented in this introductory note on insertion devices suggests the consideration of the following list of wigglers and undulators. We welcome any additional suggestions and comments.

X-Ray Ring

0.1 - 1 Å Superconducting Wiggler (Section IV) B_o = 6 T, 5 full poles, 2 half-poles

1 - 3 Å Permanent Magnet Hybrid Wiggler (Section IV) B_o = 1.5 T, 12 periods

3 - 12 Å Undulator (HXU) (Section VI.B) $\lambda_o \approx 1.5 - 3$ cm, 100 periods

5 - 50 Å Undulator (SXU) (Section VI.A) λ_o = 6 cm, 40 periods

VUV Ring

80 - 500 Å Undulator (Section V) $\lambda_o \approx 6.5$ cm, 38 periods

20 - 100 Å Permanent Magnet Hybrid Wiggler (Section V) B_o = 1 T, 12 periods

References

1. H. Winick, G. Brown, K. Halbach and J. Harris, Physics Today, p.50, May 1981.

2. J.D. Jackson, Classical Electrodynamics, (Wiley, New York), 1963.

3. Useful background material can be found in: S. Krinsky, M.L. Perlman, and R.E. Watson, Characteristics of Synchrotron Radiation and Its Sources. To appear in Handbook on Synchrotron Radiation, Vol. I, North-Holland Publishing Company (Amsterdam), Edited by E.E. Koch.

4. Our discussion follows that of E.M. Purcell, Production of Synchrotron Radiation by Wiggler Magnets, unpublished, reprinted in Proceedings Wiggler Workshop, SLAC, Eds. H. Winick and T. Knight, SSRP Report No. 77/05, 1977, p.IV-18.

5. D.F. Alferov, Yu. A. Bashmakov and E.G. Bessonov, Zh. Tekh. Fiz. 43, 2126 (1973); Eng. transl. in Sov. Phys. Tech. Phys. 18, 1336 (1974). We use the notation of S. Krinsky, Nucl. Instrum. Methods 172, 73 (1979).

6. The original analysis of undulator radiation was given by H. Motz, J. Appl. Phys. 22, 527, (1951).

7. A similar comparison was made by G. Brown, H. Winick and P. Eisenberger, The Optimization of Undulators for Synchrotron Radiation, Nucl. Instrum. and Methods (to be published).

8. See e.g. M. Sands, The Physics of Electron Storage Rings - An Introduction, Proc. Int. Sch. of Physics., E. Fermi Course No. 46, 1971, Physics with Intersecting Storage Rings, Ed. B. Touschek (Academic Press, New York), also available as Stanford Linear Accelerator Report No. SLAC-121.

9. G.K. Green, Spectra and Optics of Synchrotron Radiation, BNL 50522, 1976.

10. Use of short period undulators on low energy rings has been advocated in Ref. 7.

11. See e.g. A.M. Kondratenko and A.N. Skrinsky, Opt. Spectrosc. 42, 189 (1977).

12. K. Halbach, private communication. G. Kulipanov, private communication.

13. J.P. Blewett et al., IEEE Trans. Nucl. Sci., NS-28, 3166 (1981).

14. K. Halbach et al., ibid, 3136 (1981).

15. H. Hsieh, S. Krinsky, A. Luccio, C. Pellegrini, A. van Steenbergen, Wiggler, Undulator and Free Electron Laser Radiation Sources Development at the National Synchrotron Light Source, Proc. Int. Conf. on X-Ray and VUV Synchrotron Radiation Instrumentation, Hamburg, Germany, August 1982, to be published in Nuclear Instruments and Methods.